Check for updates

Magnetic methacrylated gelatin-*g*-polyelectrolyte for methylene blue sorption

Carla Ruiz, Myleidi Vera, [ID] Bernabé L. Rivas, Susana Sánchez and Bruno F. Urbano [ID] *

The presence of organic dyes in wastewater is a problem of growing interest due to its effect on the environment and human health. The aim of this work was to obtain magnetic hydrogels of methacrylated gelatin-*g*-polyelectrolyte to be used for the removal of methylene blue (MB) used as a model contaminant dye. Grafted gelatins with two degrees of functionalization (48% and 76%) were obtained and subsequently crosslinked using 2-acrylamido-2-methyl-1-propansulfonic acid (AMPS) and sodium 4-vinylbenzenesulfonate (SSNa) monomers. Magnetic nanoparticles were formed by an *in situ* precipitation method to easily remove the hydrogel from the adsorption medium. Our data show that the hydrogel with a low degree of methacrylation displayed a high degree of swelling and decreased stiffness due to its less connected polymer network. MB adsorption experiments showed that neither the low degree of methacrylation nor the presence of the aromatic group in the PSSNa polyelectrolyte generated an increase in the adsorption capacity of the hydrogel. However, a significant increase in the adsorption capacity was observed when dry hydrogels were combined compared to that of previously swollen hydrogel. The experimental data were non-linearly fitted to the pseudo-first and pseudo-second order models and in both cases, the highest q_e values were obtained for the GelMA-HF/PAMPS and GelMA-LF/PAMPS hydrogels. The Freundlich isotherm model was the one with the best correlation with the data ($r^2 > 0.9700$). Higher k_f values were obtained for the GelMA-HF/PAMPS and GelMA-LF/PAMPS hydrogels at 20 °C. The results obtained from this study demonstrated that magnetic polyelectrolyte-grafted gelatins are an efficient option for the removal of contaminant dyes from aqueous solutions.

1. Introduction

Organic dyes are among the main pollutants in wastewater due to their increasing use, to the point that organic dyes have become a problem of public interest.[1] It is estimated that approximately 700 000 tons of organic dyes are produced annually, and approximately 15% of these dyes are discarded in the production process, resulting in the subsequent contamination of water sources.[2] There are different types of colorants, which can be classified according to the characteristics of the chromophore. In the case of cationic dyes such as methylene blue (MB), the chromophore is in the form of a cation.[3] MB belongs to the phenothiazinium family and structurally is a heterocyclic aromatic molecule.[4] This water-soluble organic colorant is widely used in the textile, leather, dyeing, printing, coating, and plastics industries.[5,6] The concentrations of colorants in textile wastewater vary in a wide range of concentrations, with most of them reported around 50 mg L^{-1}.[7] The discharge of this compound into bodies of water is not only harmful to natural water resources but also has negative effects on human

health. This dye works by blocking the pathway for nitric oxide synthase (NOS) and soluble guanylate cyclase (sGC), which regulates smooth muscle function and vascular tone.[4] As a consequence, toxic, carcinogenic, mutagenic, and teratogenic effects are observed.[8] For this reason, it is necessary to eliminate these types of dyes present in wastewater from dyeing processes before they are discharged into water sources. The complex chemical structure of these cationic dyes makes them highly toxic and difficult to degrade by conventional wastewater treatment methods.[9]

There are different methods used for the removal of dyes in wastewater, such as membrane separation, chemical precipitation, chemical oxidation, cavitation, photocatalytic degradation, biological methods, aerobic/anaerobic treatments, and adsorption.[9–12] Among all these methods, adsorption is probably the most common method since it is a simple, efficient, ecofriendly, and low-cost technique.[13–15]

Hydrogels are three-dimensional cross-linked linear or branched hydrophilic polymers with the ability to retain large volumes of water without being dissolved.[16] Hydrogels based on biopolymers such as starch, chitosan, gelatin, agar, pectin, cellulose, and sodium alginate have received special attention due to their low cost, biodegradability, non-toxic nature, and

Departamento de Polímeros, Facultad de Ciencias Químicas, Universidad de Concepción, Concepción, Chile. E-mail: burbano@udec.cl

ease of modification.[17,18] Gelatin is a linear hydrophilic ionic polypeptide with amine, carboxylic, and alcohol functional groups, which can be used to modify the biopolymer backbone. This modification process can be performed by grafting polymer chains that allow the incorporation of new functional groups into the polymeric network.[19]

The incorporation of polyelectrolytes with an ion exchange capacity into the gelatin structure significantly increase the polarity, increasing the hydrophilicity and making the gelatin structure efficient and potentially selective towards the adsorption of polar pollutants. Various polyelectrolytes that have yielded excellent results in the removal of contaminants.[20,21] Poly(2-acrylamido-2-methyl-1-propanesulfonic acid) (PAMPS) has received special attention because its strongly ionizable sulfonate group ($-SO_3^-$) completely dissociates in the pH range of 5–7.[22] For this reason, hydrogels derived from PAMPS exhibit a swelling behavior that is independent of pH and have a great capacity to interact with cationic species.[23] These characteristics have allowed this polyelectrolyte to be an attractive material in various applications, including the development of biomaterials, sensors, supercapacitors, water purification, and agriculture.[24–26] Similarly, poly(sodium 4-vinylbenzenesulfonate) (PSSNa) is characterized as being a strong anionic electrolyte with a sulfonate group ($-SO_3^-$) that is widely used in the adsorption of contaminating cationic molecules.[27] Unlike PAMPS, PSSNa has an aromatic ring in its structure, which could be an advantage in removing pollutants that have aromatic rings. The use of hydrogels with a strong ion exchange capacity has been reported in the manufacture of metals within the three-dimensional hydrogel network, which can give the hydrogel magnetic properties, conductivity, and good adsorption capacities.[28]

Magnetic separation is a very promising method for decontamination processes since it allows the adsorbent material to be separated from the contaminated medium by the action of a magnetic field. Among the advantages of magnetic separation are the easy extraction of the adsorbent, production of no contaminants, such as flocculants, and faster treatment of large volumes of contaminated water.[29] Additionally, improvements in pollutant adsorption have been reported when magnetic particles are incorporated into hydrogels due to an improvement in electrostatic interactions.[6]

The aim of this work is to synthesize and characterize magnetic anionic polyelectrolyte-grafted hydrogels from methacrylated gelatin (GelMa) and to study their ability to remove cationic organic dyes such as MB. To this end, the gelatin will be chemically modified with methacryloyl groups, obtaining two degrees of functionalization (high and low). We hypothesize that gelatins with different degrees of functionalization (DoFs) will affect sorption; specifically, GelMA with a low DoF would present greater adsorption because: (i) it has a larger pore size (due to its lower crosslinking degree), so it has a greater capacity to retain water and dye. Then, the PAMPS and PSSNa polyelectrolytes will be grafted in the GelMA backbone, generating a crosslinked network with an anionic polyelectrolyte. In this sense, we hypothesize that a polyelectrolyte containing an aromatic moiety (PSSNa) will enhance sorption because of the

interaction between the PSSNa-MB aromatic groups. Additionally, magnetic iron oxide particles (Fe_3O_4) will be produced within the hydrogel to confer magnetics properties to the adsorbent to facilitate its separation from MB dissolution.

2. Experimental part

2.1 Material

Gelatin from porcine skin (gel strength 300, Type A), 2-acrylamido-2-methyl-1-propansulfonic acid (AMPS, 99%, Sigma-Aldrich), sodium 4-vinylbenzenesulfonate (SSNa, >90%, Sigma-Aldrich), methacrylic acid (94%), 2-hydroxy-4'-(2-hydroxyethoxy)-2-methylpropiophenone (Irgacure 2959, 98%, Sigma-Aldrich), phosphate buffered saline (PBS), sodium hydroxide, methylene blue (MB, Sigma-Aldrich), iron(III) nitrate nonahydrate (>98%), o-phthaldialdehyde (OPA, Sigma-Aldrich), deuterium oxide (D_2O, 99.9%, Sigma-Aldrich), and iron(II) sulfate heptahydrate (>99%, Merck) were used as received without any treatment if not otherwise specified.

2.2 Synthesis of GelMA

GelMA was prepared from gelatin by following a protocol previously described by Loessner D. et al.[30] Briefly, 30 g of gelatin was dissolved in 300 mL of deionized water by constant stirring in a 50 °C water bath. Then, while vigorously stirring, methacrylic anhydride (previously neutralized with sodium bicarbonate until pH = 7.4) was slowly added, and the amount added varied depending on the degree of functionalization desired: 0.6 g of anhydride per 1 g of gelatin was used for a high DoF, or 0.06 g of anhydride per 1 g of gelatin was used to obtain a low DoF. The solution was vigorously stirred for 4 h until a clear and homogeneous mixture was obtained. After this reaction period, the solution was transferred into 50 mL Falcon tubes to remove unreacted methacrylic anhydride by centrifugation (3500 rpm for 3 min). Then, the supernatant solution was diluted in a 1 : 2 ratio using preheated (40 °C) Ultrapure water. Subsequently, the GelMA was dialyzed at 40 °C for 5 days in cellulose dialysis membranes (Sigma-Aldrich, thickness 25 mm, 30 cm long). Finally, the pH of the GelMA solution was adjusted to 7.4 using NaHCO3, and the solution was lyophilized to a GelMA solid. The gelatins with high and low degrees of functionalization will identified as GelMA-HF and GelMA-LF, respectively.

2.3 Synthesis of magnetic composite hydrogels

Nanocomposite magnetic hydrogels were synthesized by starting from the protocol described by Ozay et al. with some modifications.[31] The procedure carried out was divided into two stages: (i) the synthesis of the hydrogels and (ii) the preparation of the magnetic particles inside the hydrogel (see Fig. 1). To synthesize the hydrogels, GelMA (10% w/v), Irgacure 2959 (1% w/v), and the monomer (10% w/v), which can be 2-acrylamido-2-methyl-1-propanesulfonic acid (AMPS) or sodium 4-vinyl-benzenesulfonate (SSNa), were dissolved in 3 mL of deionized water by stirring and heating the solution until complete dissolution was achieved. The mixture was transferred to Teflon
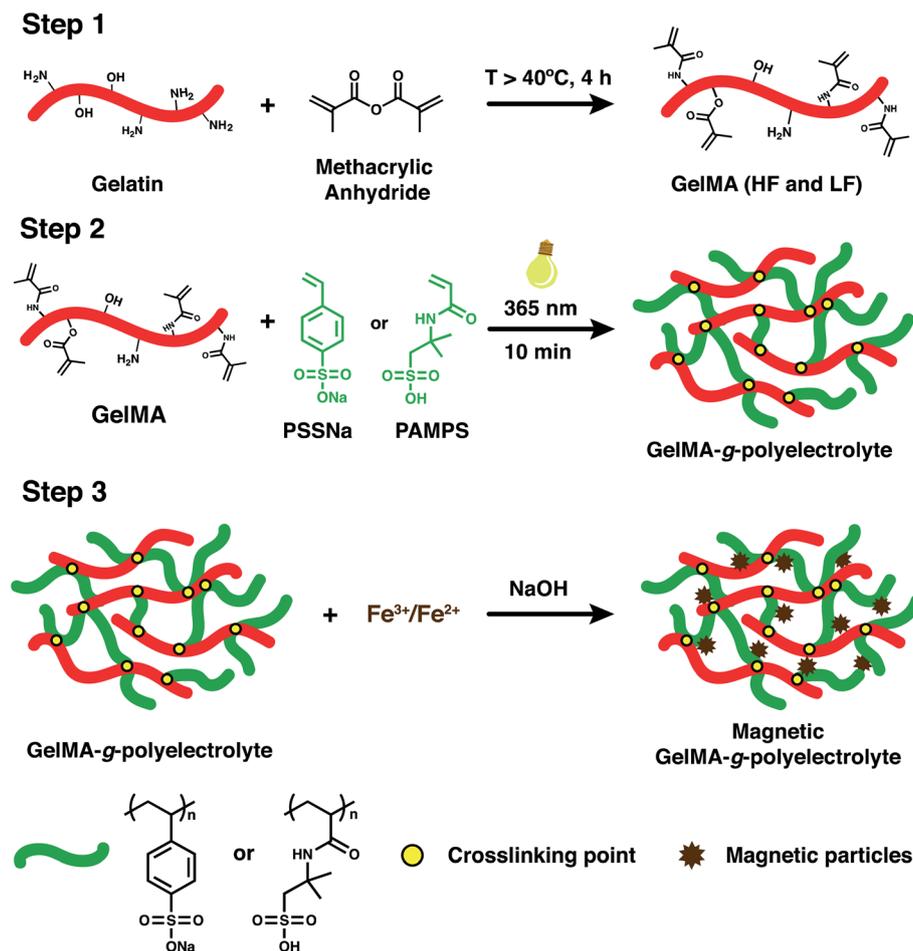
Fig. 1 Summary of the steps used for the synthesis of GelMA–based magnetic hydrogels. Step 1: methacrylation of gelatin; step 2: synthesis of GelMA-*g*-polyelectrolyte; step 3: synthesis of magnetic hydrogel.

molds with a cylindrical shape (a diameter of 8 mm and thickness of 5 mm). The precursor solution was irradiated in a photo reactor (UVP crosslinker CL-1000L, USA) for 10 min at 365 nm for crosslinking. Finally, the obtained hydrogels were allowed to cool to room temperature and removed from the mold.

The magnetic particles within the hydrogels were prepared using the precipitation method.[32] To this end, 0.40 g and 1.34 g of Fe(II) and Fe(III) were used to prepare a 0.5 mol L^{-1} solution with a Fe(II) : Fe(III) ratio of 1 : 2. The hydrogels were immersed in this solution for 15 h. Subsequently, they were washed with distilled water for 1 h, and the water was changed every 15 min to remove the unbound and/or physically adsorbed metal ions. After washing, the hydrogels loaded with metal ions were immersed in a 0.5 mol L^{-1} NaOH solution for 5 h and finally washed with PBS. Once the hydrogels were synthesized, they were dried at room temperature for 4 d. The magnetic properties of the hydrogels were evaluated by means of qualitative analysis by approaching a magnet and observing if the hydrogel adheres to the magnet.

Finally, from GelMA-HF, two types of hydrogels were obtained by grafting two types of polyelectrolytes: poly(sodium 4-vinylbenzenesulfonate) (GelMA-HF/PSSNa) and poly(2-acrylamido-2-methyl-1-propanesulfonic acid) (GelMA-HF/PAMPS). Similarly, from GelMA-LF, two types of hydrogels were obtained from the use of the two polyelectrolytes: poly(sodium 4-vinylbenzenesulfonate) (GelMA-LF/PSSNa) and the polyelectrolyte poly(2-acrylamido-2-methyl-1-propanesulfonic acid) (GelMA-LF/PAMPS).

2.4 Physicochemical characterization

FT-IR was used to study the chemical structure of gelatin, methacrylated gelatins, and the synthesized hydrogels (GelMA-HF/PSSNa, GelMA-HF/PAMPS, GelMA-LF/PSSNa, and GelMA-LF/PAMPS). A dry mass of the sample was mixed with KBr and pressed into transparent tablets that were analyzed using a spectrophotometer (NICOLET model Nexus equipped with a DTGS-KBr detector; data were collected in range of 4000–400 cm^{-1}). The methacrylation and the degree of functionalization (DoF) of gelatin was determined by ^1H NMR spectroscopy (Bruker Advance 400 MHz spectrometer) by analyzing a dissolution of GelMA 33 mg mL^{-1} in D_2O. The calculation of the DoF was made by comparing the proton signals at $\delta = 2.9$ ppm (the

protons of the methylene group of lysine) for the unmodified gelatin and GelMA,[33] according to the following equation:

$$\text{DoF} = \left(1 - \frac{\text{lysine methylene proton of GelMA}}{\text{lysine methylene proton of gelatin}}\right) \times 100\% \tag{1}$$

Additionally, the DoF was confirmed by a fluorescent method based on the labeling of the NH_2 groups using the *o*-phthaldialdehyde reagent solution (OPA). For this, 350 μL of a 0.5 mg mL^{-1} GelMA solution in PBS was mixed with 700 μL of OPA. Unmethacrylated gelatin in PBS was used as a blank, and a calibration curve was collected between 0.02 and 1.0 mg mL^{-1}. All the measurements were made at 50 °C by measuring the fluorescence intensity at $\lambda_{em} = 450$ nm with $\lambda_{ex} = 360$ nm (Photon Technology International, QuantaMaster, USA). The DoF was determined by analyzing the GelMA samples and using the following equation:[30]

$$\text{DoF} = \frac{0.5 - X}{0.5} \times 100\% \tag{2}$$

where 0.5 corresponds to the concentration of the compared samples, *i.e.*, the concentrations of gelatin, GelMA-HF and GelMA-LF, and X corresponds to the residual amine concentration (X mg mL^{-1}) determined from the calibration curve.

Hydrogel swelling was carried out by contacting the dry hydrogels with 50 mL of distilled water at room temperature for 24 h. The hydrogel weight was taken at different intervals after drying with filter paper to remove the excess water on the surface. All measurements were made in triplicate. The swelling ratio (S_w) was determined using the following equation:

$$S_w = \frac{w_S}{w_d} \tag{3}$$

where w_S is the weight of the hydrogel swollen at time t, and w_d is the weight of the dried hydrogel at time zero.

The rheological properties of the hydrogels were tested using a rheometer (TA Instrument, DHR-3, USA). The storage (G') and loss (G'') moduli were determined by performing oscillatory strain sweeps using parallel plates with an 8 mm geometry and a strain range of 0.01% to 500% at 25 °C.

The morphological, surface, and composition characteristics of the hydrogels were studied by scanning electron microscopy (SEM, JEOL JSM-6380LV, Germany) and energy dispersive X-ray spectroscopy (EDS). For the analysis, the hydrogels were dried by lyophilization and subsequently coated with gold under a reduced pressure (SPI-Module sputter coater).

2.5 Sorption studies

These studies were carried out using the dye MB. First, the adsorption kinetics was studied, and the hydrogels were immersed in 10 mL of a 3.0 mg L^{-1} solution of MB at 20 °C and pH of 7.4. At different time intervals, an aliquot of the supernatant (1 mL) was taken, and the absorbance was measured. After that, batch experiments were conducted using two methods: (i) the dry hydrogels were placed in contact with the dye solution, and (ii) the previously swollen hydrogels were placed in contact with the dye solution. The general procedure used for the adsorption studies consisted of contacting the hydrogels with 10 mL of a dye (3 mg L^{-1}) for 48 h. To evaluate the kinetic performance, the experimental data were non-linearly fitted to the pseudo- first and pseudo-second order model, as expressed by the following equations:

Pseudo-first model:

$$q_t = q_e(1 - e^{-k_1 t}) \tag{4}$$

Pseudo-second model:

$$q_t = \frac{k_2 q_e^2 t}{1 + k_2 q_e t} \tag{5}$$

where k_1 and k_2 is the pseudo-first and pseudo-second-order rate constant, respectively, and q_e and q_t represent the amount of dye adsorbed (mg g$_{dry\ hydrogel}^{-1}$) at equilibrium and at time t, respectively.

In addition, sorption isotherms were collected. To this end, solutions with variable concentrations in the range of 0.1–50 mg L^{-1} were prepared from a stock solution with a concentration of 50 mg L^{-1}. The experiments were carried out by the batch method, in which 10 mL of the different dye solutions were contacted with a constant mass of hydrogel during 24 h using an orbital shaker with temperature control (Heidolph, Unimax 1010). The experiments were carried out at 20, 30, and 40 °C. The experimental data was studied using the Langmuir, Freundlich, and Temkin isotherm model expressed according to following equations:[34]

Langmuir:

$$q_e = \frac{Q_0 b C_e}{1 + b C_e} \tag{6}$$

Freundlich:

$$q_e = k_f C_e^{1/n} \tag{7}$$

Temkin:

$$q_e = \frac{RT}{b_T} \ln A_T C_e \tag{8}$$

where q_e is the equilibrium adsorption of the hydrogel (mg$_{dye}$ g$_{hydrogel}^{-1}$), C_e is the equilibrium concentration (mg L^{-1}), Q_0 is the maximum monolayer sorption capacity (mg$_{dye}$ g$_{hydrogel}^{-1}$), b is the Langmuir constant (L mg^{-1}) associated with the free energy of sorption. For Freundlich isotherm, k_f is the Freundlich constant which is associated with the efficiency of adsorption, and n is a dimensionless parameter that indicates the favorability of adsorption. For Temkin isotherm, b_T is related to the heat of sorption (J mol^{-1}) and A_T is the Temkin isotherm constant (L mg^{-1}).

The dye concentration in all of the experiments was determined before and after contact with the hydrogels by performing absorbance measurements at the maximum wavelength, λ_{max} (660 nm), using a UV-vis spectrophotometer (Thermo-Fisher Scientific, AQUAMATE). The dye calibration curve was obtained with 12 measurements for concentrations ranging

from 0.5 to 15 mg L^{-1}. All experiments were performed in triplicate.

One-way analysis of variance (ANOVA) with Tukey's *post hoc* test was performed to obtain the significant difference between samples. Statistical significance was designated with *$p < 0.05$, **$p < 0.01$, and ***$p < 0.001$.

3. Results and discussion

3.1 Synthesis of GelMA

Methacrylation consists of polymerizable groups incorporated into gelatin chains to allow interactions among groups and the formation of chemical hydrogels, which are more stable than physical hydrogels. Gelatin is composed of diverse amino acid residues depending on the hydrolysis procedure and the source of the proteins. In general, the functional groups suitable to be methacrylated are hydroxyls group (*e.g.*, serine, hydroproline, and hydroxylysine) and amino groups (*e.g.*, lysine and hydroxylysine).[35]

Fig. 2 shows the spectroscopic characterization and comparison of gelatin and the methacrylated gelatins GelMA-LF and GelMA-HF as evidence for the effectiveness of functionalization. The FTIR spectra of the three molecules (see Fig. 2a) have in common a broad band with a medium intensity at 3500 cm^{-1} (attributed to the stretching vibration of N–H and O–H bonds) and bands at 2941 cm^{-1} corresponding to the C–H stretching vibration. The main difference between the FTIR spectra of the gelatins, with respect to the GelMA-HF and

GelMA-LF, is the presence of a high-intensity sharp band at approximately 1649 cm^{-1} corresponding to the C=O bond stretching vibration. This band is slightly more intense for GelMA-HF than for GelMA-LF, which is consistent with for GelMA-HF having a higher degree of functionalization. Other evidence of functionalization is the shift in the broad band at 3466 cm^{-1} to 3302 cm^{-1}, which is characteristic of the N–H bond stretching vibration for *N,N*-substituted amides.[36]

Fig. 2b shows a comparison of the ^{1}H-NMR spectra obtained for gelatin, GelMA-LF and GelMA-HF. The spectra of the GelMA-LF and GelMA-HF hydrogels present two signals that are absent in the gelatin spectrum at $\delta = 5.4$ and 5.7 ppm, which were assigned to the vinyl protons of the grafted methacryloyl groups. The signal at $\delta = 1.9$ ppm in the two modified gelatin spectra are attributed to the protons of the methyl group of the grafted methacryloyl group, which further confirms functionalization. Additionally, a decrease in the intensity of the lysine methylene signal at $\delta = 2.9$ ppm is observed as the degree of functionalization (DoF) increased. These findings confirm the modification of gelatin to GelMA and agree well with similar previously published studies.[37–39]

The DoF is of critical importance since it would affect the crosslinking sites between gelatin chains needed for polyelectrolyte grafting. The DoF of the modified gelatins was determined by ^{1}H NMR (see Fig. 2b). The increase in the signal intensity at $\delta = 5.4$ and 5.7 ppm (the protons of the methacrylate vinyl group) and the decrease in the signal intensity at $\delta = 2.9$ ppm (the protons of the methylene group of lysine) were
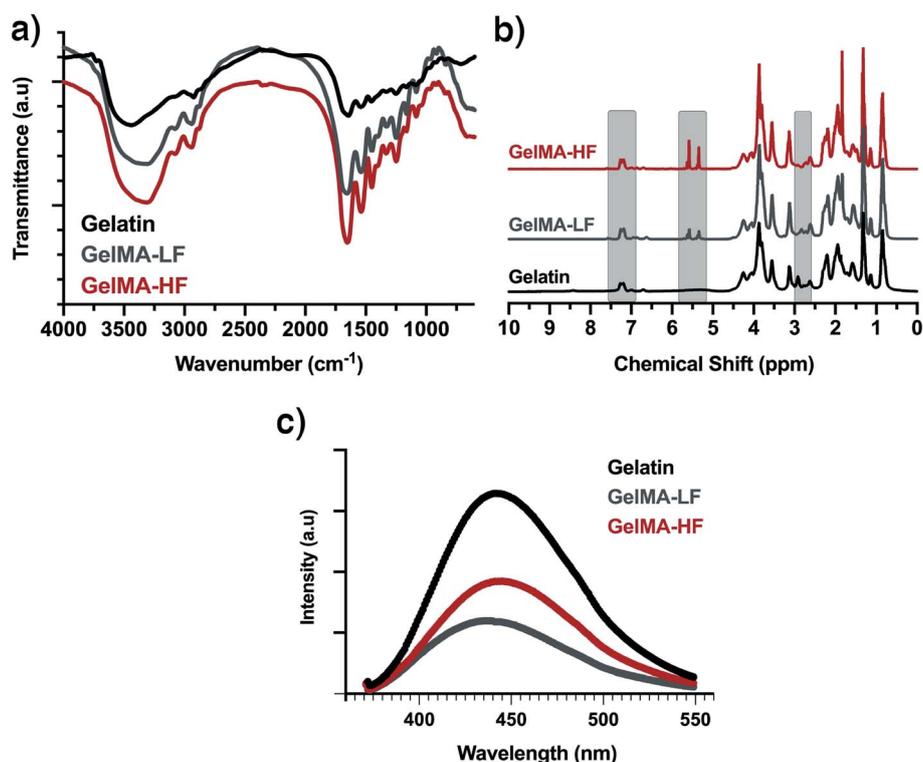

Fig. 2 Characterization of gelatin and methacrylated gelatin: (a) FTIR, (b) ^{1}H-NMR, (c) fluorescence spectra (the gelatin and GelMA concentrations are 0.5 mg mL^{-1}).

used to confirm the modification of the gelatin to GelMA. Since the signal of the gelatin aromatic amino acids, between $\delta = 6.9$ and 7.5 ppm, did not change, their intensity was used to normalize the intensity of other protons in the samples. The calculation of the DoF was made by comparing the proton signals at $\delta = 2.9$ ppm of the unmodified gelatin and GelMA, according to eqn (1). The DoF obtained for GelMA-HF and GelMA-LF were 73% and 43%, respectively.

In addition, the DoF was confirmed using a reagent solution of the fluorescent molecule phthaldialdehyde (OPA), which was used in a procedure described by Loessner *et al.*[30] In this experiment, the remaining NH$_2$ groups were labeled with the OPA reagent, a fluorescent dye with a blue emission (see Fig. 2c). Although we observed the GelMA spectrum to shift relative to the gelatin spectrum, we were able to prepare a calibration curve by measuring the intensity at 450 nm. The DoF was determined by using the eqn (2). The DoF values obtained were 76% for GelMA-HF and 48% for GelMA-LF. These degrees of functionalization are consistent with those obtained through ^{1}H NMR, and consequently, the two functionalization ratios are confirmed.

3.2 Characterization of the hydrogel

The incorporation of the polyelectrolytes PAMPS and PSSNa into the GelMA hydrogel chain was confirmed by FTIR (see Fig. 3a). The broad band at 3400 cm^{-1} was attributed to the

stretching vibration of N–H and O–H bonds due to the possible presence of water in the hydrogels. The band at 2930 cm^{-1} is due to C–H stretching vibrations. All the spectra also show a high-intensity sharp band at 1650 cm^{-1} corresponding to the C=O stretching vibration of the amides. This band is more intense in the polymers that have PAMPS in their structure due to the high concentration of carbonyl groups in the polymer chains. The main difference observed in the spectra for polymers having PSSNa is the presence of overtones or a set of weak bands at 2000–2400 cm^{-1} corresponding to the aromatic compounds.[36,40] Based on the results obtained from the FTIR spectra, it is possible to confirm the incorporation of the polyelectrolytes in the GelMA chain.

Hydrogels were evaluated to determine their water absorption capacity (eqn (3)) as a function of time (see Fig. 3b). As a general observation, the degree of swelling was greater in hydrogels with a low DoF. The low DoF of the hydrogels reduced the density of crosslinking networks and promoted the formation of large pores capable of hosting a greater volume of water.[33] Interestingly, it was observed that the hydrogels with PSSNa and an aromatic moiety in their structure presented a higher swelling ratio than the hydrogels with PAMPS. The driving force in swelling involves different contributions, such as difference in the osmotic pressure between the solution inside the hydrogel and the bulk solution, charge repulsion forces of the sulfonate groups "pumping" water into the
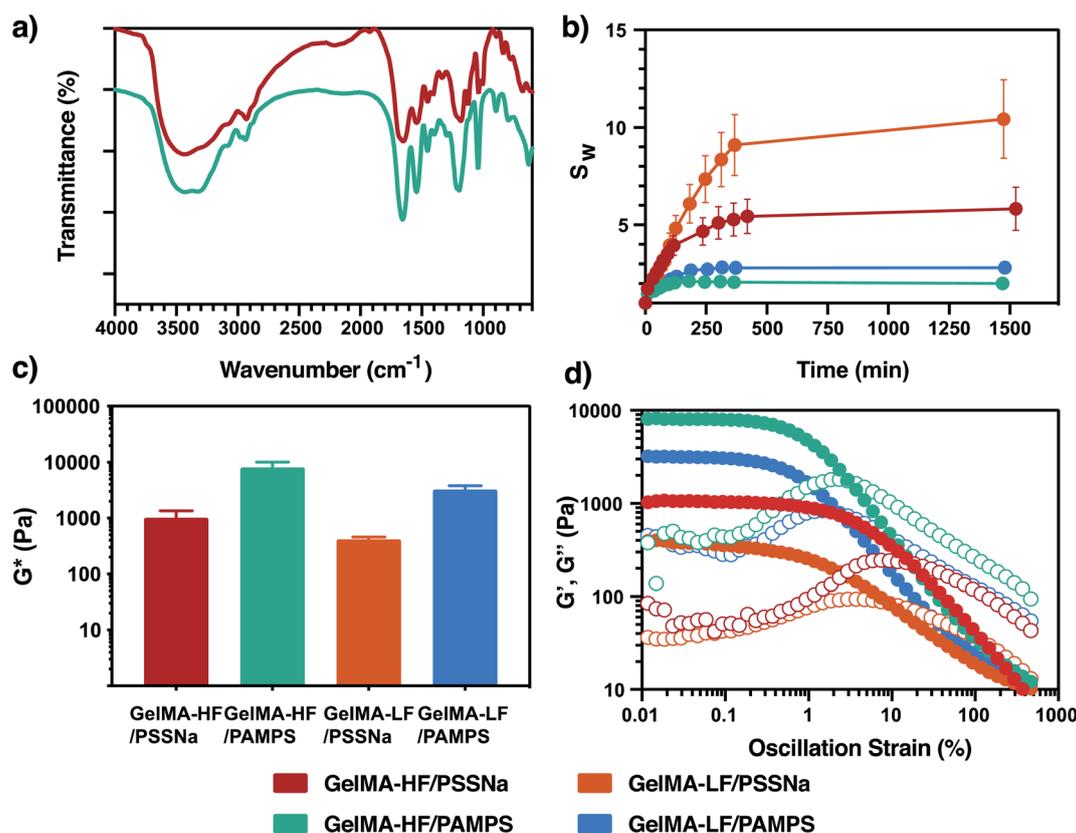

Fig. 3 Characterization of the polyelectrolyte-grafted GelMA hydrogel: (a) representative FTIR spectra of GelMA-HF/PSSNa and GelMA-HF/PAMPS, (b) swelling behavior (pH 7.4, 20 °C), (c) complex modulus (gap 1000 μm, determined at a strain of 0.01% and temperature of 25 °C), and (d) oscillatory shear strain assays (gap 1000 μm, 25 °C).

hydrogel, and hydrophilicity of the pendant groups. In our system, both structures contain hydrophilic sulfonate groups, but the chemical structure where these groups are attached differs. It has been reported that PAMPS displays a more hydrophobic character than PSSNa due to the aliphatic branches on its pendant groups,[41] which could explain the larger sorption of the PSSNa polyelectrolyte.

The mechanical strength of the hydrogels was evaluated by rheology tests. Fig. 3c shows the complex modulus, G^* ($G^* = \sqrt{G'^2 + G''^2}$),[42] obtained for the samples. The high functionalized gelatin (GelMA-HF) showed a greater modulus than GelMA-LFs, which is due to the higher degree of methacrylation generating a large number of crosslinking points and, consequently, a high rigidity. These results are consistent with the swelling studied since the greater degree of crosslinking is associated with a lower swelling degree and greater stiffness. The oscillatory shear strain assay (see Fig. 3d) performed with a low deformation showed that all the hydrogels display a G' that is independent of the applied strain, the so-called linear viscoelastic region (LVR). The strain at which the modulus drops (γ_c) corresponds to the elastic limit where the microstructure of the polymer begins to be altered irreversibly. Moreover, it is observed that the gelatins grafted with PAMPS have a higher stiffness and are less strain resistant (decreased γ_c) than PSSNa-based hydrogels, exhibiting a steep decrease in the modulus at 0.5% strain, which is consistent with a more brittle structure (see Fig. 3d).[43]

The SEM images of the GelMA hydrogels are displayed in Fig. 4. The morphology of freeze-dried hydrogels does not show the presence of superficial pores, and on the contrary, a rough surface is shown in all the hydrogels analyzed. This could be attributed to the presence of PSSNa and PAMPS in the structure of GelMA hydrogels, since as reported by Gan, *et al.*, the incorporation of polymer chains to GelMA hydrogels affects its microstructure, resulting in a loss of superficial porosity, as observed in Fig. 4a.[44] Additionally, the elemental analysis was performed at the hydrogel surfaces by using energy dispersive X-ray spectroscopy (EDS) to determine the concentration of the elements S and Fe coming from sulfonate groups and magnetic particles, respectively (see Fig. 4c and d). The K-α line centered at 6.4 keV, which is attributed to Fe, confirms the presence of iron oxide particles in the hydrogel. Additionally, the elemental analysis revealed that the iron content is high in the hydrogels prepared with GelMA having a high DoF. This can be explained by the fact that the incorporation of magnetic particles into the hydrogel is performed through the interaction of the anionic sulfonate groups with the ferric and ferrous cations, which are oxidized to form the magnetic particles. Although it is expected that highly functionalized gelatins have a greater number of polyelectrolyte chains compared to low-functionalized ones, the concentration of sulfur is similar in all of the hydrogels, so the high concentration of Fe is not explained by the sulfonate groups. We believe that GelMA-HF retains the iron ions during washing better than GelMA-LF because GelMA-HF contains more crosslinking points, leading to more magnetic particles.
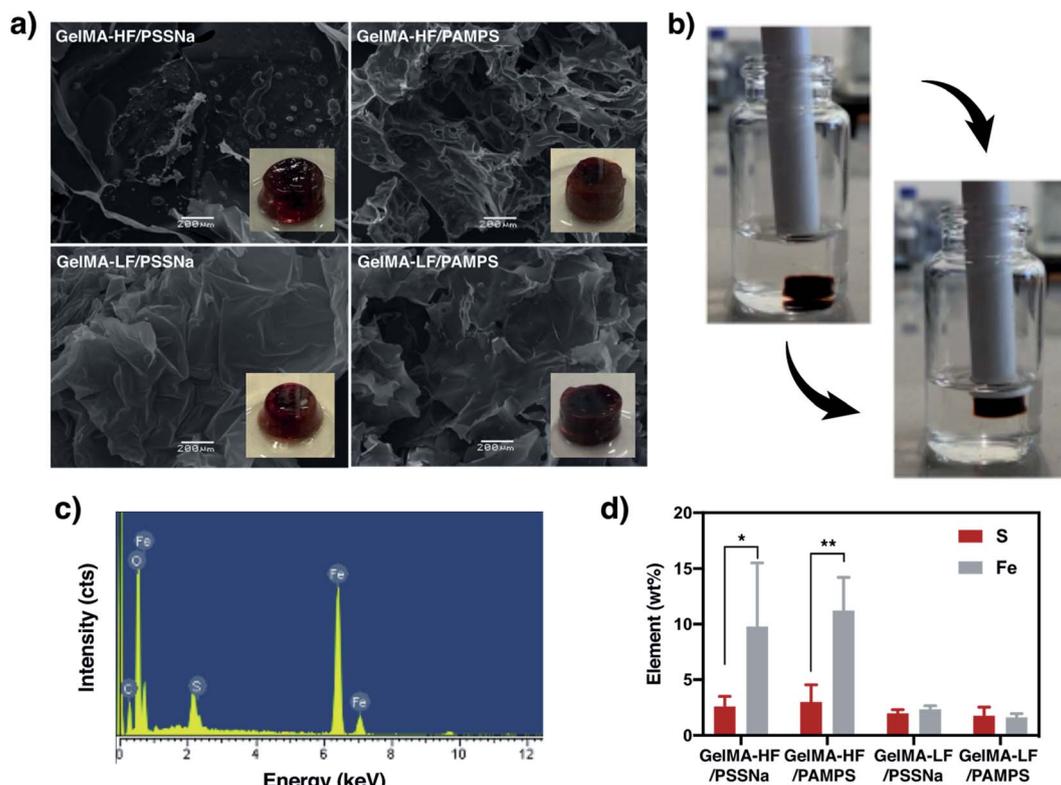

Fig. 4 (a) SEM images of the polyelectrolyte GelMA hydrogels, (b) verification of the magnetic properties of the hydrogels, (c) representative EDS analysis (d) concentration (wt%) of S and Fe determined by EDS ($n \geq 3$).

Finally, the magnetic properties of the hydrogels were verified with a magnet, as shown in Fig. 4b. It can be verified that all the synthesized GelMA hydrogels react to the presence of the magnetic field, which will be very promising for magnetic separation.

3.3 Sorption studies

To evaluate the potential ability of magnetic hydrogels to remove organic contaminants, we used methylene blue dye as a test molecule. This dye consists of an aromatic heterocyclic compound with a positive charge. In this way, the positive charge can interact electrostatically with the sulfonate groups, while the aromatic group can establish $\pi-\pi$ interactions with side groups that also have aromatic groups, such as PSSNa. To determine the nature of the predominant hydrogel–dye interaction, adsorption studies were performed by contacting both dry and previously swollen hydrogels with the dye solution. Using dry adsorbents, the sorption capacity is mainly due to the swelling process of the hydrogel, where the analyte accesses the hydrogel together with the water molecules, leading to a predominant physical sorption. On the contrary, when previously swollen hydrogels are used, the sorption capacity due to swelling is minimized, and sorption is mainly due to the interaction between the functional groups of the hydrogels and the analyte.[45,46] The results of MB sorption are shown in Fig. 5. First, in the dry state, GelMA-LF/PSSNa exhibited better sorption than GelMA-HF/PSSNa. This can be ascribed to the low

crosslinked nature of GelMA-LF/PSSNa, enabling it to host more water and dye molecules (see Fig. 5a). Secondly, the GelMA-LF/PAMPS hydrogel presents better adsorption of dye than the PSSNa hydrogel, suggesting that aromatic moieties did not influence sorption. Thirdly, it was observed that previously swollen hydrogels have a lower capacity for dye sorption than a dry adsorbent, and no significant differences were observed between the gelatins with high and low degrees of functionalization, neither for PSSNa nor PAMPS. These results indicate that the swelling process greatly influences dye sorption by increasing the sorption capacity. With these results, the following sorption experiments were carried out using the GelMA/PAMPS hydrogels. Fig. 5b shows the MB adsorption kinetics. This study was carried out using the batch method to determine the optimal contact time in which the hydrogels reach equilibrium. In this case, dry hydrogels were contacted with the MB solution, very fast sorption was observed. The same trend is observed for all hydrogels, reaching maximum removal after 50 min of contact. Similarly, as seen in Fig. 5a, the GelMA/PAMPS hydrogel displayed the highest adsorption capacity. To reveal the differences in the kinetic performance, the experimental data were non-linearly fitted to the pseudo- first and pseudo-second order models (eqn (4) and (5)). The rate constants and the amount of dye adsorbed at equilibrium q_e resulted from the model fit are given in Table 1. The models were fitted with the data in the time range of 0–30 min to avoid the methodological bias of using q_t data at the equilibrium.[47]
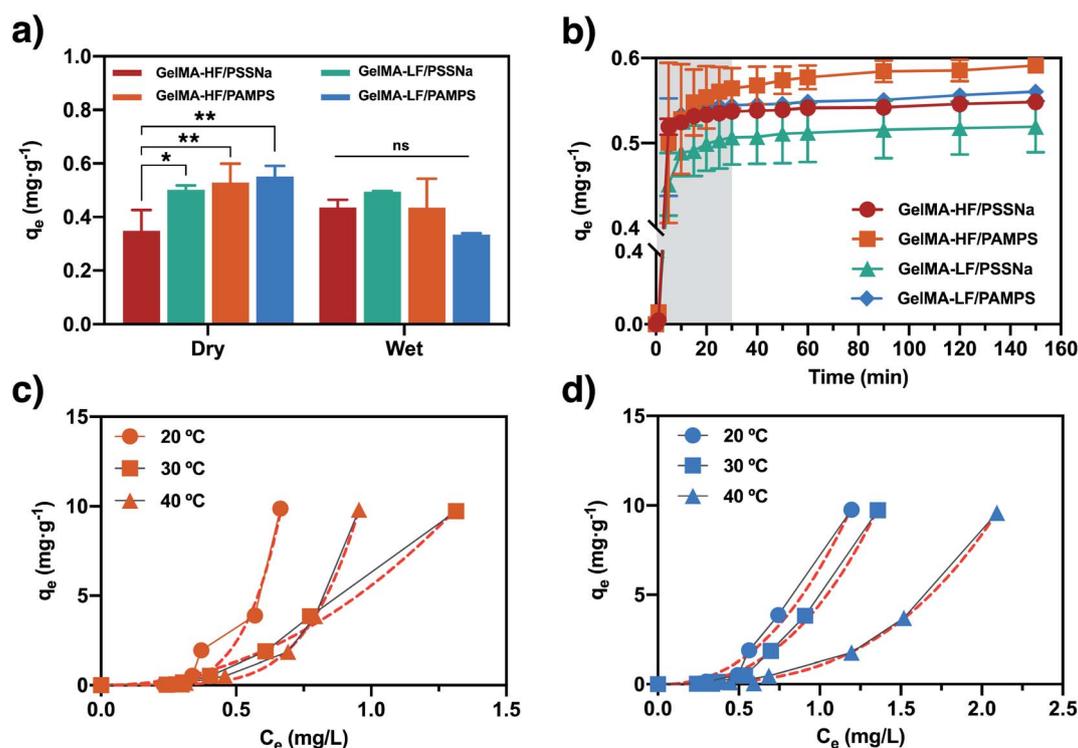
Fig. 5 Adsorption of MB by the GelMA composite hydrogel: (a) comparison of the dry and wet hydrogel sorption behaviors ([MB] = 3.0 mg L^{-1}, pH = 7.4, 20 °C, 100 rpm, n = 3), (b) sorption kinetics, where the dashed lines corresponds to the pseudo-second order fit ([MB] = 3.0 mg L^{-1}, pH = 7.4, 20 °C, 100 rpm), (c) sorption isotherms of GelMA-HF/PAMPS, and (d) sorption isotherms of GelMA-LF/PAMPS, where the dashed lines correspond to the Freundlich isotherm model fit (pH = 7.4, 20 °C, 100 rpm).

Table 1 Kinetics parameters of MB adsorption onto GelMA composite hydrogels

Pseudo-first order	k_1 (min^{-1})	q_e (mg g$_{dry\ hydrogel}$$^{-1}$)	r^2
GelMA-HF/PSSNa	0.31 ± 0.01	0.54 ± 0.001	0.9409
GelMA-HF/PAMPS	0.30 ± 0.06	0.56 ± 0.03	0.9712
GelMA-LF/PSSNa	0.31 ± 0.03	0.50 ± 0.03	0.9763
GelMA-LF/PAMPS	0.28 ± 0.03	0.550 ± 0.005	0.9430
Pseudo-second order	k_2 (g$_{dry\ hydrogel}$ mg^{-1} min^{-1})	q_e (mg g$_{dry\ hydrogel}$$^{-1}$)	r^2
GelMA-HF/PSSNa	0.56 ± 0.02	0.620 ± 0.004	0.9065
GelMA-HF/PAMPS	0.54 ± 0.10	0.65 ± 0.02	0.9464
GelMA-LF/PSSNa	0.65 ± 0.09	0.57 ± 0.03	0.9498
GelMA-LF/PAMPS	0.48 ± 0.07	0.640 ± 0.009	0.9107

Both models address to the same conclusions, all of the hydrogels exhibit similar rate constants, and some slight differences in q_e are observed. Nevertheless, both models indicated that GelMA/PAMPS hydrogels exhibit a slightly higher sorption capacity in agreement with those determined previously (see Fig. 5a).

Adsorption isotherms provide valuable information regarding the adsorption process of the MB dye by the hydrogel. Based on the results obtained in the previous experiments, the isotherms were obtained only for the hydrogels with PAMPS and by using hydrogels previously swollen in water. In this way, the swelling effect of the solvent is minimized, and the adsorption of the dye can be attributed to the interactions between the MB molecules and the polymer. Fig. 5c and d show the equilibrium experiments carried out at the temperatures of 20, 30, and 40 °C using MB solution in the range of 0.1–50 mg L^{-1} based on previous report about the concentration of these type of pollutants in textile wastewater effluents.[7,48,49] Differently from the usual shape of the curves when solvent absorption plays an important role,[50,51] the present systems exhibits a convex shape ascribed to the previously equilibrated hydrogels in water. The isotherm indicated that at a low concentration of MB, the sorption process is not favorable, while at a high concentration, the sorption capacity exhibits a steep increase attributed to the increment of concentration gradient. To provide more insight about the sorption process the experimental data were fitted to diverse isotherm models, namely Langmuir, Freundlich, and Temkin (see eqn (6)–(8)). The isotherm parameters obtained are displayed in Table 2. The Langmuir parameters clearly indicate the model does not fit the experimental data, while Temkin model gave very low correlation coefficient, only Freundlich model gave an adequate correlation ($r^2 > 0.9700$). The Freundlich isotherm model is expressed according to eqn (7). The higher the k_f value, the higher the affinity of the hydrogel with the dye. Both GelMA-HF/PAMPS and GelMA-LF/PAMPS have high values of k_f and n at 20 °C, which demonstrated that

Table 2 Freundlich, Langmir and Temkin isotherm parameters

Isotherm	Temperature	Isotherm parameter	GelMA-HF/PAMPS	GelMA-LF/PAMPS
Langmuir^a	20 °C	b (L mg^{-1})	-1.93 ± 0.08	-1.32 ± 0.03
		Q_0 (mg$_{dye}$ g$_{hydrogel}$$^{-1}$)	-0.08 ± 0.02	-0.12 ± 0.03
		r^2	0.6330	0.6594
	30 °C	b (L mg^{-1})	-1.28 ± 0.06	-1.14 ± 0.06
		Q_0 (mg$_{dye}$ g$_{hydrogel}$$^{-1}$)	-0.12 ± 0.02	-0.09 ± 0.02
		r^2	0.5778	0.6214
	40 °C	b (L mg^{-1})	-1.33 ± 0.03	-0.86 ± 0.16
		Q_0 (mg$_{dye}$ g$_{hydrogel}$$^{-1}$)	-0.10 ± 0.01	-0.12 ± 0.04
		r^2	0.6467	0.6031
Freundlich	20 °C	k_f (L mg^{-1})	71.9 ± 0.9	6.50 ± 0.01
		n	0.203 ± 0.001	0.427 ± 0.001
		r^2	0.9708	0.9858
	30 °C	k_f (L mg^{-1})	5.560 ± 0.007	4.47 ± 0.01
		n	0.477 ± 0.005	0.389 ± 0.001
		r^2	0.9904	0.9951
	40 °C	k_f (L mg^{-1})	12.41 ± 0.04	1.04 ± 0.01
		n	0.198 ± 0.001	0.198 ± 0.001
		r^2	0.9989	0.9994
Temkin	20 °C	b_T (J mol^{-1})	273 ± 46.87	403.68 ± 62.28
		A_T (L mg^{-1})	3.47 ± 0.21	3.01 ± 0.23
		r^2	0.7959	0.8113
	30 °C	b_T (J mol^{-1})	430.94 ± 27.42	408.90 ± 31.45
		A_T (L mg^{-1})	3.01 ± 0.20	2.50 ± 0.11
		r^2	0.8995	0.8081
	40 °C	b_T (J mol^{-1})	419.64 ± 36.80	555.94 ± 62.86
		A_T (L mg^{-1})	2.19 ± 0.04	1.91 ± 0.27
		r^2	0.6648	0.6810

^{a} Negative values of Q_0 and b has no physical sense.

a higher affinity is achieved at low temperatures. The values obtained in this study indicate that both hydrogels are good absorbents and the values obtained for n and k_f are comparable with those reported in the literature for the absorption of MB.[52,53] In addition, and contrary to our hypothesis, a high DoF hydrogel displays a greater affinity than a low DoF hydrogel for methylene blue (higher k_f). To explain this, we need to consider that, besides sulfonate groups, iron oxide particles can adsorb MB molecules as well.[54] In particular, GelMA-HF/PAMPS possesses a higher concentration of Fe than GelMA-LF/PAMPS (see Fig. 5c). In addition, the reported pH point of zero charge (pHpzc) of Fe_3O_4 is approximately 6.5;[55] thus, at pH > pHpzc, the surfaces of particles are predominantly negatively charged, whereas at pH < pHpzc, the surfaces are predominately positively charged. Hence, electrostatic interactions between methylene blue and the inorganic particles can exist at the pH of the sorption experiments (7.4).

In summary, the results indicate that for dry hydrogels, water absorption has significant influence allowing access to solvated dye molecules resulting in predominantly physical and rapid adsorption. Moreover, when used, hydrogels prehydrated adsorption capacity decreases. The interaction between dye molecules and hydrogels is primarily electrostatic, with no effect of the aromatic groups in the polyelectrolyte (PSSNa), with a potential contribution of iron oxide particles.

4. Conclusions

In this study, methacrylated gelatins with two degrees of functionalization (approximately 48% and 76%) were synthetized and confirmed by ^{1}H-NMR and fluorescence spectroscopy. From the methacrylated gelatins, magnetic composite hydrogels were obtained with two types of grafted anionic polyelectrolytes: PAMPS and PSSNa. The hydrogel with a low degree of methacrylation displayed a higher swelling and lower stiffness than the hydrogel with a high degree of methacrylation, which ascribed to the less connected polymer network. The MB sorption experiment revealed that the hydrogels display a moderate sorption capacity; however, we demonstrated that neither a low degree of methacrylation nor the aromatic group in the PSSNa polyelectrolyte enhanced the sorption capacity. Overall, the hydrogels exhibited greater sorption when the dry hydrogels were contacted with the dye solution (compared with previously swollen ones), fast sorption, and a great affinity for MB at low temperatures. Finally, these swollen hydrogels can subsequently be removed from the adsorption medium by the action of a magnetic field. In this way, we envision that the obtained magnetic hydrogels can be applied to remove other cationic contaminants as well as in the treatment of waters contaminated with dye residues.

Conflicts of interest

There are no conflicts to declare.

Acknowledgements

References

1   A. Pardo, H. Garcia, P. Ramirez, M. A. Carrillo-Alvarado, K. S. Krishna, N. Dominguez, M. T. Islam, H. Wang and J. C. Noveron, Self-regenerating photocatalytic hydrogel for the adsorption and decomposition of methylene blue and antibiotics in water, *Environ. Technol. Innov.*, 2018, **11**, 321–327.

2   J. Xing, B. Yang, Y. Shen, Z. Wang, F. Wang, X. Shi and Z. Zhang, Selective removal of acid fuchsin from aqueous solutions by rapid adsorption onto polypyrrole crosslinked cellulose/gelatin hydrogels, *J. Dispersion Sci. Technol.*, 2019, **40**, 1591–1599.

3   G. V. Brião, S. L. Jahn, E. L. Foletto and G. L. Dotto, Highly efficient and reusable mesoporous zeolite synthetized from a biopolymer for cationic dyes adsorption, *Colloids Surf., A*, 2018, **556**, 43–50.

4   L. P. Nguyen and N. S. Gerstein, Cardiovascular Pharmacology in Noncardiac Surgery, in *Essentials of Cardiac Anesthesia for Noncardiac Surgery*, Elsevier, 2019, pp. 247–288.

5   Y. Wu, L. Zhang, C. Gao, J. Ma, X. Ma and R. Han, Adsorption of copper ions and methylene blue in a single and binary system on wheat straw, *J. Chem. Eng. Data*, 2009, **54**, 3229–3234.

6   A. Pourjavadi, S. H. Hosseini, F. Seidi and R. Soleyman, Magnetic removal of crystal violet from aqueous solutions using polysaccharide-based magnetic nanocomposite hydrogels, *Polym. Int.*, 2013, **62**, 1038–1044.

7   D. Yaseen and M. Scholz, Textile dye wastewater characteristics and constituents of synthetic effluents: a critical review, *Int. J. Environ. Sci. Technol.*, 2019, **16**, 1193–1226.

8   G. Babaladimath and V. Badalamoole, Silver nanoparticles embedded pectin-based hydrogel: a novel adsorbent material for separation of cationic dyes, *Polym. Bull.*, 2019, **76**, 4215–4236.

9   A. Raj, B. Bethi and S. H. Sonawane, Investigation of removal of crystal violet dye using novel hybrid technique involving hydrodynamic cavitation and hydrogel, *J. Environ. Chem. Eng.*, 2018, **6**, 5311–5319.

10 A. Pal, S. Pan and S. Saha, Synergistically improved adsorption of anionic surfactant and crystal violet on chitosan hydrogel beads, *Chem. Eng. J.*, 2013, **217**, 426–434.

11 P. Manikandan, P. Palanisamy, R. Baskar and P. Sakthisharmila, Influence of Chemical Structure of Reactive Blue (Diazo), Direct Red (Diazo) and Acid Violet (Triaryl Alkane) Dyes on the Decolorization Efficiency by Photo Assisted Chemical Oxidation Process (PACO), *Int. J. Eng. Technol. Res.*, 2017, **5**(1), 01–14.

12 R. Foroutan, R. Mohammadi, J. Razeghi and B. Ramavandi, Performance of algal activated carbon/Fe$_3$O$_4$ magnetic composite for cationic dyes removal from aqueous solutions, *Algal Res.*, 2019, **40**, 101509.

13 K. Junlapong, P. Maijan, C. Chaibundit and S. Chantarak, Effective adsorption of methylene blue by biodegradable superabsorbent cassava starch-based hydrogel, *Int. J. Biol. Macromol.*, 2020, **158**, 258–264.

14 R. R. Mohamed, M. H. A. Elella, M. W. Sabaa and G. R. Saad, Synthesis of an efficient adsorbent hydrogel based on biodegradable polymers for removing crystal violet dye from aqueous solution, *Cellulose*, 2018, **25**, 6513–6529.

15 R. Foroutan, R. Mohammadi and B. Ramavandi, Elimination performance of methylene blue, methyl violet, and Nile blue from aqueous media using AC/CoFe$_2$O$_4$ as a recyclable magnetic composite, *Environ. Sci. Pollut. Res.*, 2019, **26**, 19523–19539.

16 Ö. B. Üzüm, G. Çetin, S. Kundakcı and E. Karadağ, Swelling and dye adsorption properties of polyelectrolyte semi-IPNs including of acrylamide/(3-acrylamidopropyl) trimethyl ammonium chloride/poly (ethylene glycol), *Sep. Sci. Technol.*, 2019, 1–13.

17 K. Kaur and R. Jindal, Comparative study on the behaviour of Chitosan-Gelatin based Hydrogel and nanocomposite ion exchanger synthesized under microwave conditions towards photocatalytic removal of cationic dyes, *Carbohydr. Polym.*, 2019, **207**, 398–410.

18 S. J. Peighambardoust, O. A. Bavil, R. Foroutan and N. Arsalani, Removal of malachite green using carboxymethyl cellulose-g-polyacrylamide/montmorillonite nanocomposite hydrogel, *Int. J. Biol. Macromol.*, 2020, **159**, 1122–1131.

19 S. Sethi, B. S. Kaith, M. Kaur, N. Sharma and S. Khullar, A hydrogel based on dialdehyde carboxymethyl cellulose–gelatin and its utilization as a bio adsorbent, *J. Chem. Sci.*, 2020, **132**, 1–16.

20 T. H. Tran, H. Okabe, Y. Hidaka and K. Hara, Removal of metal ions from aqueous solutions using carboxymethyl cellulose/sodium styrene sulfonate gels prepared by radiation grafting, *Carbohydr. Polym.*, 2017, **157**, 335–343.

21 A. M. Farag, H. H. Sokker, E. M. Zayed, F. A. N. Eldien and N. M. A. Alrahman, Removal of hazardous pollutants using bifunctional hydrogel obtained from modified starch by grafting copolymerization, *Int. J. Biol. Macromol.*, 2018, **120**, 2188–2199.

22 E. Su and O. Okay, Hybrid cross-linked poly (2-acrylamido-2-methyl-1-propanesulfonic acid) hydrogels with tunable viscoelastic, mechanical and self-healing properties, *React. Funct. Polym.*, 2018, **123**, 70–79.

23 I. Clara, R. Lavanya and N. Natchimuthu, pH and temperature responsive hydrogels of poly (2-acrylamido-2-methyl-1-propanesulfonic acid-co-methacrylic acid): synthesis and swelling characteristics, *J. Macromol. Sci., Part A: Pure Appl.Chem.*, 2016, **53**, 492–499.

24 E. Cevik, A. Bozkurt, M. Hassan, M. A. Gondal and T. F. Qahtan, Redox-mediated poly (2-acrylamido-2-methyl-1-propanesulfonic acid)/ ammonium molybdate hydrogels for highly effective flexible supercapacitors, *ChemElectroChem*, 2019, **6**, 2876–2882.

25 S. ÇAVUŞ, Y. Kaya, Z. Gonder, G. GÜRDAĞ and I. Vergili, *Removal of Cu (II), Ni (II) and Zn (II) from aqueous solutions using poly (2-acrylamido-2-methyl-1-propanesulfonic acid) gel: sorption kinetics and characterization*, 2018.

26 F. Wang, J.-H. Jeon, S.-J. Kim, J.-O. Park and S. Park, An eco-friendly ultra-high performance ionic artificial muscle based on poly (2-acrylamido-2-methyl-1-propanesulfonic acid) and carboxylated bacterial cellulose, *J. Mater. Chem. B*, 2016, **4**, 5015–5024.

27 Y. Ono, I. Nakase, A. Matsumoto and C. Kojima, Rapid optical tissue clearing using poly (acrylamide-co-styrenesulfonate) hydrogels for three-dimensional imaging, *J. Biomed. Mater. Res., Part B*, 2019, **107**, 2297–2304.

28 N. Sahiner, In situ metal particle preparation in cross-linked poly (2-acrylamido-2-methyl-1-propansulfonic acid) hydrogel networks, *Colloid Polym. Sci.*, 2006, **285**, 283–292.

29 Z. S. Pour and M. Ghaemy, Removal of dyes and heavy metal ions from water by magnetic hydrogel beads based on poly (vinyl alcohol)/carboxymethyl starch-g-poly (vinyl imidazole), *RSC Adv.*, 2015, **5**, 64106–64118.

30 D. Loessner, C. Meinert, E. Kaemmerer, L. C. Martine, K. Yue, P. A. Levett, T. J. Klein, F. P. Melchels, A. Khademhosseini and D. W. Hutmacher, Functionalization, preparation and use of cell-laden gelatin methacryloyl–based hydrogels as modular tissue culture platforms, *Nat. Protoc.*, 2016, **11**, 727.

31 O. Ozay, S. Ekici, Y. Baran, N. Aktas and N. Sahiner, Removal of toxic metal ions with magnetic hydrogels, *Water Res.*, 2009, **43**, 4403–4411.

32 O. Ozay, S. Ekici, Y. Baran, S. Kubilay, N. Aktas and N. Sahiner, Utilization of magnetic hydrogels in the separation of toxic metal ions from aqueous environments, *Desalination*, 2010, **260**, 57–64.

33 X. Li, S. Chen, J. Li, X. Wang, J. Zhang, N. Kawazoe and G. Chen, 3D culture of chondrocytes in gelatin hydrogels with different stiffness, *Polymers*, 2016, **8**, 269.

34 M. A. Al-Ghouti and D. A. Da'ana, Guidelines for the use and interpretation of adsorption isotherm models: a review, *J. Hazard. Mater.*, 2020, **393**, 122383.

35 K. Yue, X. Li, K. Schrobback, A. Sheikhi, N. Annabi, J. Leijten, W. Zhang, Y. S. Zhang, D. W. Hutmacher, T. J. Klein and A. Khademhosseini, Structural analysis of photocrosslinkable methacryloyl-modified protein derivatives, *Biomaterials*, 2017, **139**, 163–171.

36 D. L. Pavia, G. M. Lampman, G. S. Kriz and J. A. Vyvyan, *Introduction to spectroscopy*, Cengage Learning, 2008.

37 M. Zhou, B. H. Lee and L. P. Tan, *A dual crosslinking strategy to tailor rheological properties of gelatin methacryloyl*, 2017.

38 E. Hoch, C. Schuh, T. Hirth, G. E. Tovar and K. Borchers, Stiff gelatin hydrogels can be photo-chemically synthesized from low viscous gelatin solutions using molecularly functionalized gelatin with a high degree of

methacrylation, *J. Mater. Sci.: Mater. Med.*, 2012, **23**, 2607–2617.

39 K. Yue, X. Li, K. Schrobback, A. Sheikhi, N. Annabi, J. Leijten, W. Zhang, Y. S. Zhang, D. W. Hutmacher and T. J. Klein, Structural analysis of photocrosslinkable methacryloyl-modified protein derivatives, *Biomaterials*, 2017, **139**, 163–171.

40 J. Li, Y. Chen, Y. Yin, F. Yao and K. Yao, Modulation of nano-hydroxyapatite size via formation on chitosan–gelatin network film in situ, *Biomaterials*, 2007, **28**, 781–790.

41 I. Moreno-Villoslada, C. Torres, F. González, T. Shibue and H. Nishide, Binding of Methylene Blue to Polyelectrolytes Containing Sulfonate Groups, *Macromol. Chem. Phys.*, 2009, **210**, 1167–1175.

42 C. W. Macosko, *Rheology: Principles, Measurements, and Applications*, Wiley-VCH, Inc., 1994.

43 C. Solar, D. Palacio, S. Sánchez and B. F. Urbano, Oscillatory strain sweeps of hydrogels from methacrylated alginate macromonomers: assessment of synthesis and acquisition variables, *J. Chil. Chem. Soc.*, 2019, **64**, 4542–4546.

44 D. Gan, T. Xu, W. Xing, M. Wang, J. Fang, K. Wang, X. Ge, C. W. Chan, F. Ren and H. Tan, Mussel-inspired dopamine oligomer intercalated tough and resilient gelatin methacryloyl (GelMA) hydrogels for cartilage regeneration, *J. Mater. Chem. B*, 2019, **7**, 1716–1725.

45 T. Singh and R. Singhal, Kinetics and thermodynamics of cationic dye adsorption onto dry and swollen hydrogels poly (acrylic acid-sodium acrylate-acrylamide) sodium humate, *Desalin. Water Treat.*, 2015, **53**, 3668–3680.

46 J. Fan, Z. Shi, M. Lian, H. Li and J. Yin, Mechanically strong graphene oxide/sodium alginate/polyacrylamide nanocomposite hydrogel with improved dye adsorption capacity, *J. Mater. Chem. A*, 2013, **1**, 7433–7443.

47 J.-P. Simonin, On the comparison of pseudo-first order and pseudo-second order rate laws in the modeling of adsorption kinetics, *Chem. Eng. J.*, 2016, **300**, 254–263.

48 D. Sivakumar, Role of Lemna minor Lin. in treating the textile industry wastewater, *Int. J. Environ. Ecolog. Geol. Mining Eng.*, 2014, **8**, 55–59.

49 M. F. Abid, M. A. Zablouk and A. M. Abid-Alameer, Experimental study of dye removal from industrial wastewater by membrane technologies of reverse osmosis and nanofiltration, *Iran. J. Environ. Health Sci. Eng.*, 2012, **9**, 17.

50 C. O. Panão, E. L. Campos, H. H. Lima, A. W. Rinaldi, M. K. Lima-Tenório, E. T. Tenório-Neto, M. R. Guilherme, T. Asefa and A. F. Rubira, Ultra-absorbent hybrid hydrogel based on alginate and SiO2 microspheres: a high-water-content system for removal of methylene blue, *J. Mol. Liq.*, 2019, **276**, 204–213.

51 X.-S. Hu, R. Liang and G. Sun, Super-adsorbent hydrogel for removal of methylene blue dye from aqueous solution, *J. Mater. Chem. A*, 2018, **6**, 17612–17624.

52 Ö. Gökçe Kocabay and O. İsmail, Acrylamide based hydrogels in swelling and uptake of methylene blue from aqueous solutions, *Main Group Chem.*, 2019, **18**, 281–290.

53 W. Wang, Y. Zhao, H. Bai, T. Zhang, V. Ibarra-Galvan and S. Song, Methylene blue removal from water using the hydrogel beads of poly (vinyl alcohol)-sodium alginate-chitosan-montmorillonite, *Carbohydr. Polym.*, 2018, **198**, 518–528.

54 P. Zhang, D. O'Connor, Y. Wang, L. Jiang, T. Xia, L. Wang, D. C. W. Tsang, Y. S. Ok and D. Hou, A green biochar/iron oxide composite for methylene blue removal, *J. Hazard. Mater.*, 2020, **384**, 121286.

55 M. Kosmulski, The pH-dependent surface charging and points of zero charge: V. Update, *J. Colloid Interface Sci.*, 2011, **353**, 1–15.